



# Carbon nanotubes enhancement of tribological and nanomechanical properties of PVDF-BN nanocomposites

Uwa O. Uyor<sup>1,3</sup> · Abimbola P. I. Popoola<sup>1</sup> · Olawale M. Popoola<sup>2,3</sup>

Received: 30 July 2023 / Revised: 7 February 2024 / Accepted: 12 February 2024  
© The Author(s) 2024

## Abstract

There have been continuous efforts to further promote various properties of polymeric materials to meet various industrial demands, especially in the area of thermal, electrical, mechanical and wear properties. This study developed polyvinylidene fluoride (PVDF)-boron nitride (BN) nanocomposites and significantly enhanced their wear and nanomechanical properties by incorporating very low content of carbon nanotubes (CNT). The nanocomposites were developed via simple technique of solution mixing and hot compression. Scanning electron microscope showed that the nanocomposites achieved uniform microstructure with no significant agglomeration of the nanoparticles in the PVDF matrix. The wear rate of PVDF-10wt%BN-0.1wt%CNT was reduced from  $5.68 \times 10^{-4}$  and  $5 \times 10^{-3}$  mm<sup>3</sup>/Nm for pure PVDF to  $1.6 \times 10^{-6}$  and  $8 \times 10^{-6}$  mm<sup>3</sup>/Nm at applied loads of 10 N and 20 N, respectively. Also, an increase in hardness and elastic modulus of 225% and 219% for PVDF-10wt%BN-0.1wt%CNT was obtained relative to the pure PVDF at 100-mN applied load. While the nanocomposite showed about 75% and 103% increments compared to PVDF-10wt%BN at 100 mN. This study revealed that the addition of small amount of CNT could further improve the wear and mechanical properties of PVDF-BN as well as any other polymer-ceramic binary systems various advanced engineering applications.

**Keywords** PVDF · Nanomechanical · Tribological · CNT · Boron nitride

---

✉ Uwa O. Uyor  
UyorUO@tut.ac.za

<sup>1</sup> Department of Chemical, Metallurgical and Materials Engineering, Tshwane University of Technology, Private Bag X680, Pretoria, South Africa

<sup>2</sup> Department of Electrical Engineering, Tshwane University of Technology, Private Bag X680, Pretoria, South Africa

<sup>3</sup> Center for Energy and Electrical Power, Tshwane University of Technology, Private Bag X680, Pretoria, South Africa

## Introduction

Polymers are organic compounds that are characterized by interconnected networks of molecular chains, mainly hydrogen and carbon atoms. They are also characterized by their lightweights, ease of fabrication, resistance to chemical attacks, low electrical and thermal conductivity, etc. Hence, polymers usually find applications in the industries such as automobiles, energy storage [1], machine components, fabrication of biomaterials, etc. Polyvinylidene fluoride (PVDF) is a semicrystalline polymer characterized by appreciable thermal stability, high pyroelectric and piezoelectric properties and good resistance to chemical attacks [2]. These characteristics, along with the material's good elasticity and simplicity in modification, made it excellent polymer for several technological applications [2]. However, PVDF as well as other polymers such as polypropylene, epoxy resin, polyester resin, etc., have features of low mechanical strength, hardness and wear resistance, thereby limiting their applications in the industries.

The need for advanced polymer-based materials to meet various advanced engineering applications has led to the use of different nanofillers such as metallic, ceramic, carbon-based nanofillers, etc., as reinforcements in polymer matrix to enhance mechanical strength, anti-wear, thermal stability, energy-related properties, etc. [3, 4]. Recently, 2D materials such as graphene have made significant contribution in enhancing properties of composite materials due to their exceptional engineering features [5]. For instance, graphene is a type of carbon-based nanoparticle that exists in a two-dimensional hexagonal shape. It is composed of  $sp^2$  hybridized carbon [6] and has a honeycomb crystal structure [7, 8]. The nanoparticle's substantial aspect ratio, minuscule size, large surface area [9] and interconnected structure contribute significantly to its ability to enhance the characteristics of polymers, even when present in very low concentrations. Shen et al. [10] and Li et al. [11] have reported a reduction in wear rate of around 94.1% and 75%, respectively, by adding only about 0.5 wt% and 0.7 wt% of graphene to epoxy and nylon-6.

In addition, Wang et al. [12] fabricated nanocomposites by incorporating few layer graphene flakes into PVDF and assessed their mechanical properties using the nanoindentation technique. With a loading of 1.0 wt% in the PVDF matrix, the authors observed a significant increase in both the elastic modulus and hardness, measuring approximately 337% and 228%, respectively. Similarly, Shokrieh et al. [13] observed a 35% increase in elastic modulus and a 25% rise in hardness when 0.5 wt% of graphene nanoplatelets were added. On the other hand, hexagonal boron nitride (BN) has received tremendous attention in the past years as 2D and advanced engineering material [14–16]. When polymers are reinforced with a considerably amount of BN nanofillers, the resultant nanocomposites give an improved properties such as hardness, anti-wear, thermal stability, etc. [17–19]. According to a study by Joy et al. [19], BN/epoxy nanocomposites demonstrated a greater storage modulus than clean epoxy. Abe et al. [20] showed an improvement in the hardness, elastic modulus and wear properties of boron nitride-reinforced titanium alloy matrix composites.

However, large amount of BN nanofillers is often needed to significantly impact on the properties of the fabricated polymer composites. This limits the flexibility of such composite materials, at the same time increase the weight of the composite materials. To address these shortcomings, this study developed PVDF-based composites containing low BN content (5 wt% and 10 wt%) with small addition of carbon nanotubes (CNT) (0.05 wt% and 0.1 wt%) to achieved significant increase in wear and mechanical properties without deteriorating the flexibility of the nanocomposites. This is as the result of the lightweight, high aspect ratios, large surface areas, good mechanical and thermal properties of the CNTs [21], which are desired features to improve polymers' properties [22–25]. Despite the numerous works on polymer-BN and polymer-CNT composites for enhancing various engineering properties of polymers, there are limited works on the hybrid design of polymer-BN-CNT ternary nanocomposites for advanced tribological and nanomechanical properties. The PVDF-BN-CNT ternary nanocomposites developed in this study showed better mechanical and tribological properties compared to the pure PVDF and its PVDF-BN binary counterpart. This is credited to the high aspect ratio and large surface area of the CNT in combination with the desired features of BN, which promoted mechanical interlocking of the PVDF molecular chains and enhanced homogenous distribution of the nanoparticles in the polymer matrix.

## Experimental method

### Materials

Polyvinylidene fluoride (PVDF) (MW: 534,000 and density: 1.74 g/mL at 25 °C) in addition to *N,N*-dimethyl formamide (DMF) (assay:  $\geq 99\%$ ) was bought from Sigma-Aldrich, South Africa. Hexagonal boron nitride (BN) (assay:  $> 99.5\%$ , particles size:  $< 100$  nm and density: 2.2 g/mL at 25 °C) and multi-walled carbon nanotubes (MWCNT) (purity:  $> 98\%$ , diameter: 10–30 nm and length: 5–20  $\mu\text{m}$ ) were purchased from Hongwu International Group, China. All the materials were used as received without further modification.

### Polymer nanocomposites fabrication

The polymer nanocomposites were prepared using solution mixing process. To exfoliate the nanoparticles, different concentrations of the BN (5 wt% and 10 wt%) and the CNT (0.05 wt% and 0.1 wt%) were mixed at random in beakers containing 100 mL of DMF. The mixtures were ultrasonicated (using SCIENTECH bath Ultrasonicator with a model code; 704, India) for 5 h at a high frequency, 300 W power and 80 °C temperature. PVDF (100 wt%, 94.95 wt%, 94.9 wt%, 89.95 wt%, 89.9 wt%, 95 wt% and 90 wt%) was dissolved in a 200 mL of DMF and magnetically stirred for 10 min at a speed of 300 rpm and temperature of 80 °C using magnetic stirrer (model code; SKU: CSLDHOTSTIR, UK). The dispersed mixtures of BN and CNT were then combined with the pre-dispersed PVDF and stirred thoroughly for

3 h. After that, the mixtures were poured on a clean glass plate and dried in an air circulating oven (model code; SFE 600, Czech Republic). Then, the nanocomposites were hot pressed to 25-mm diameter and 1.5-mm thickness for 10 min at 200 °C and pressure of 10 MPa using a carver press molder (model code; C 3851, USA) and cool to 25 °C at a rate of 10 °C/min. The schematic illustration of the nanocomposite fabrication process is shown in Fig. 1. The nanocomposites developed for this study with various concentrations of BN and CNT include PVDF-5wt%BN-0.05wt%CNT, PVDF-10wt%BN-0.05wt%CNT, PVDF-5wt%BN-0.1wt%CNT, PVDF-10wt%BN-0.1wt%CNT, PVDF-5wt%BN and PVDF-10wt%BN. For comparison, pure PVDF was also produced using the same procedures described above.

## Characterization and measurement

Diffraction patterns of both BN and CNT nanofillers as well as fabricated nanocomposites were studied using X-ray diffraction (XRD) (X'pert PRO PANalytical, UK) at 30 kV and 40 mA. The XRD investigation was carried out using Cu K $\alpha$  radiation at 25 °C. A scanning electron microscope (SEM) (VEGA 3 TESCAN, Czech Republic) working at accelerated voltage of 20 kV was utilized to examine the agglomeration of the nanoparticles and morphology of the nanocomposites. The surfaces of the samples were first coated with carbon film using vacuum carbon coater (Q300T ES, USA) to make them conductive for the SEM analysis. In compliance with ASTM G99-95 standard, a tribometer (Anton Paar TRB<sup>3</sup>, Austria) was used to evaluate the wear response of the nanocomposites. At temperature of 25 °C, a dry sliding rotating module with a pin-on-disk configuration was used for the wear test for 15 min at applied loads of 10 N and 20 N and sliding speed of 0.06 m/s. A stainless steel ball with a radius of 0.3 cm and a roughness of 0.03  $\mu\text{m}$  (Ra) was employed as

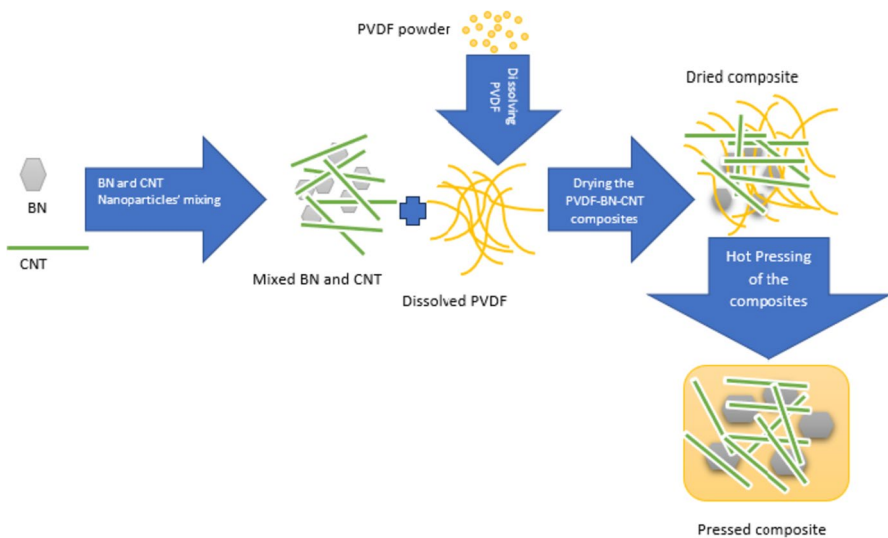


**Fig. 1** Schematic illustration of the nanocomposites' fabrication route

the counterface. The nanocomposites' coefficient of friction was measured, and the wear rate was determined using profilometer (Surtronic S128, Austria) attached to the tribometer. In accordance with ASTM D785 standard, the nanomechanical characteristics were assessed using nanoindenter (Anton Paar TTX-NHT3, Austria). The nanoindenter was operated at 100-mN and 300-mN applied loads, 20-s penetration time, 20-s holding period and 20-s release time. For repeatability, this study measured ten nanoindentation tests at different locations for each sample, and average of the ten nanoindentations per sample is presented. The wear and nanoindentation tests were conducted without any surface preparation of the samples.

## Results and discussion

### XRD analysis

X-ray diffraction patterns of the nanoparticles are shown in Fig. 2. Different diffraction peaks corresponding to hexagonal structure of BN at  $2\theta=26.4^\circ$ ,  $41.6^\circ$ ,  $49.9^\circ$ ,  $54.9^\circ$  and  $75.8^\circ$  were present as previously studied [26–28]. The CNT showed major diffraction peaks at  $2\theta=26.4^\circ$  and  $42.5^\circ$  which correspond to graphitic diffraction peaks of CNT [29]. Both the BN and CNT nanoparticles showed similar diffraction peaks, which emanated from their hexagonal crystal structures [26], and this aids for

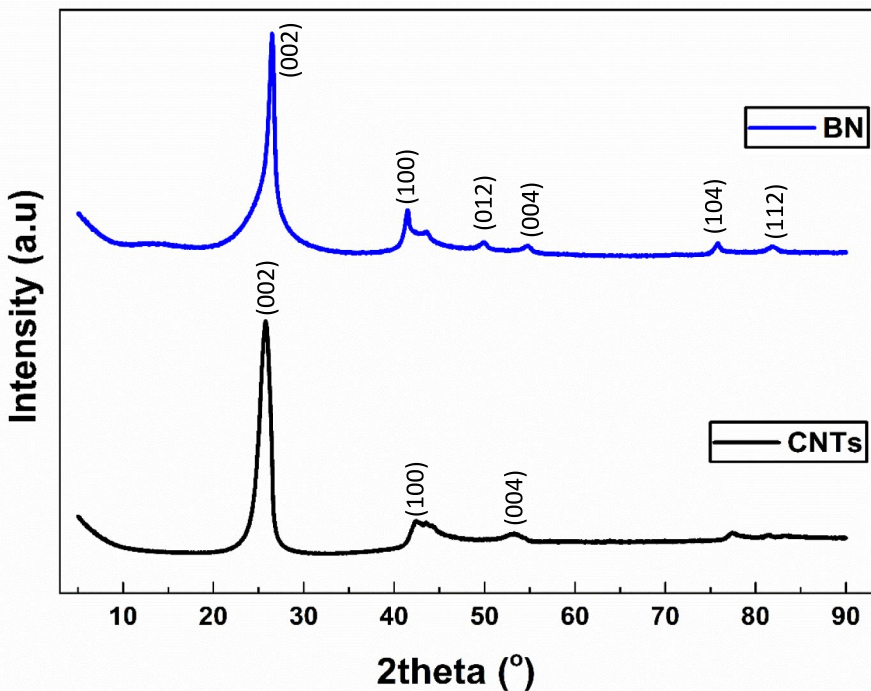


Fig. 2 X-ray diffraction of the nanoparticles

the compatibility of BN and CNT nanoparticles since they have similar crystal structure [29]. The X-ray diffraction patterns of the nanocomposites are shown in Fig. 3. The pure PVDF has diffraction peaks corresponding to  $\alpha$ -phase at  $2\theta = 17.5^\circ, 19.0^\circ, 26.0^\circ$  and  $37.5^\circ$ , which represent (100), (020), (110) and (021) crystal planes [30]. The broad diffraction peak at  $2\theta = 37.5^\circ$  with crystal plane of (021) decreased with the addition of the nanoparticles for the developed nanocomposites in this study. This is expected since the nanoparticles in the PVDF matrix can facilitate heterogeneous nucleation, where they can act as nucleation agents with increase in phase change [31, 32].

### Microstructural analysis

SEM micrographs of the pure PVDF and its nanocomposites are shown in Fig. 4. The pure PVDF showed a smooth surface and homogeneous microstructure in Fig. 4a. The SEM micrographs of all the nanocomposites revealed dense morphologies, which resulted from the presence of BN in the nanocomposites. The BN is a 2D structural material; hence, the PVDF-5wt%BN and PVDF-10wt%BN nanocomposites showed layered microstructure as presented in Fig. 4b and c, respectively. There is no observable agglomeration of the BN nanoparticles in the PVDF matrix, possibly due to the use of the BN at relatively low concentration. Also, the PVDF-BN-CNT-based nanocomposites show no significant clustering of the nanofillers in the

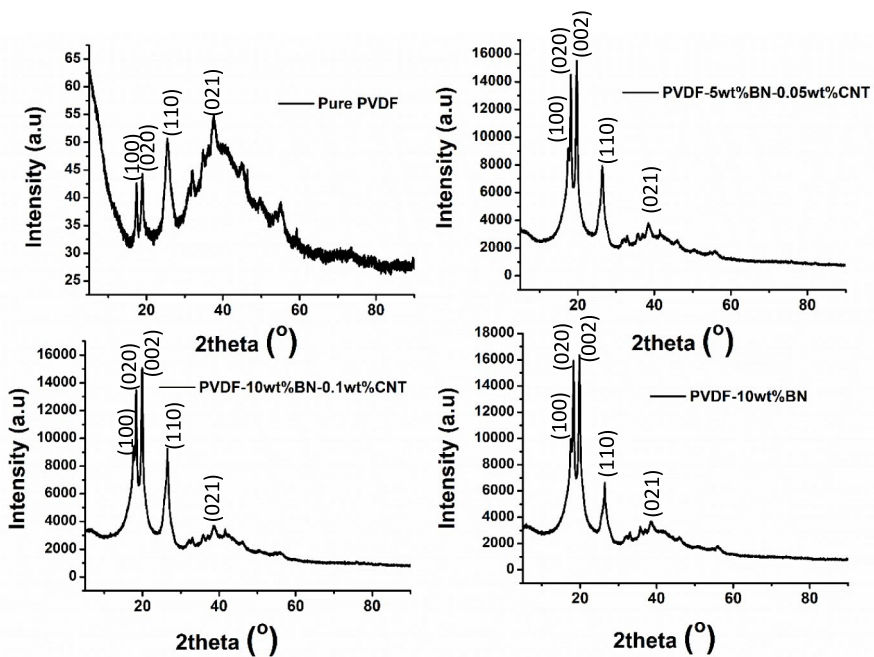
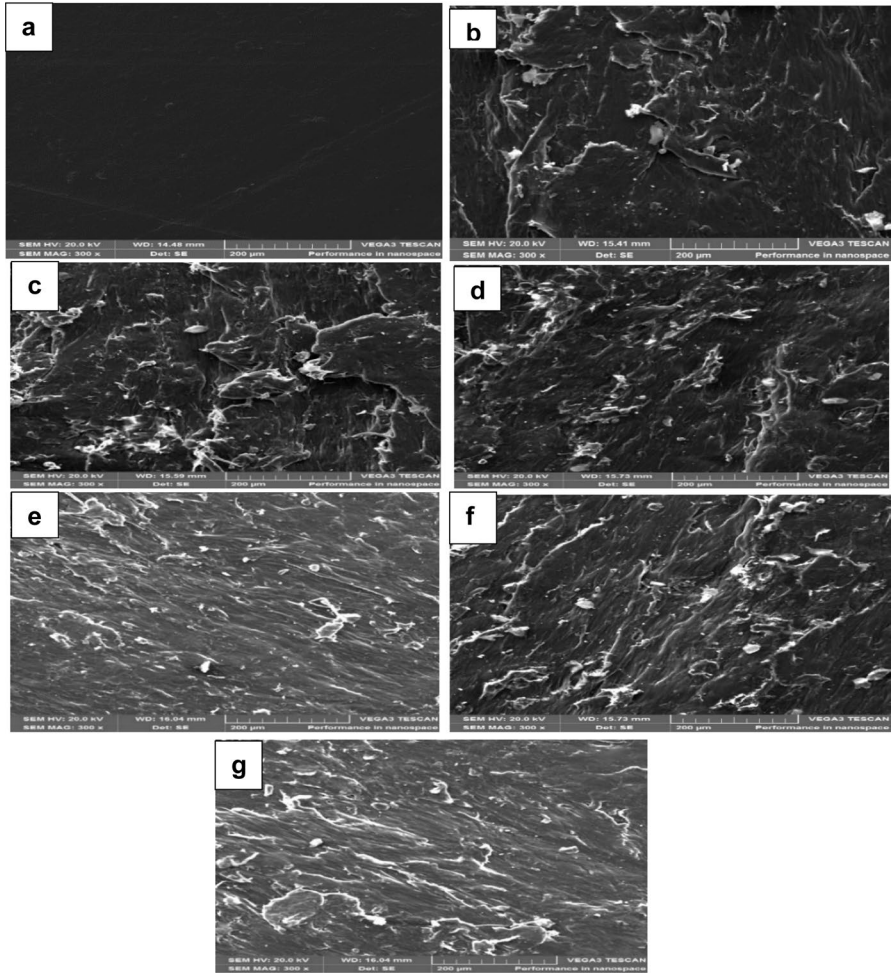


Fig. 3 X-ray diffraction of the nanocomposites



**Fig. 4** SEM micrographs of **a** pure PE, **b** PE-5wt%BN, **c** PE-10wt%BN, **d** PE-5wt%BN-0.05wt%CNT, **e** PE-10wt%BN-0.05wt%CNT, **f** PE-5wt%BN-0.1wt%CNT and **g** PE-10wt%BN-0.1wt%CNT nanocomposites

PVDF matrix as depicted in Fig. 4d-g. The nanocomposites revealed uniform microstructure and dense morphology, especially for PVDF-10wt%BN-0.05wt%CNT and PVDF-10wt%BN-0.1wt%CNT nanocomposites. The absence of the formation of small bundles or clustering of the nanoparticles in the PVDF-BN-CNT systems is due to the BN and CNT assisting each other in distribution in the polymer matrix, where walls-to-walls contacts of CNT are minimized by the presence of BN, and layers-to-layers contacts of BN are minimized by CNT. There was no significant agglomeration of the nanoparticles in the polymer matrix, indicating good synergy between the hybrid ceramic and carbon-based nanoparticles as previously reported [33]. The CNT has a great tendency of showing agglomeration in the polymer

matrix; however, the presence of the BN aided in its distribution. The nanocomposites displayed no substantial microcracking and debonding of the nanoparticles from the matrix, thereby indicating good compatibility of the constituent nanoparticles. The unnoticed agglomeration of the nanoparticles in the PVDF matrix contributed to the improved nanomechanical properties and wear resistance in this study.

### Tribological properties

The plot of coefficient of friction (CoF) against sliding time for the pure PVDF and its nanocomposites at applied loads of 10 N and 20 N is shown in Fig. 5. The addition of the nanoparticles greatly reduced the CoF of the pure PVDF as observed for both 10 N and 20 N applied loads. For instance, at sliding time of 800 s, the CoF reduced from 0.36 and 0.33 for pure PVDF to 0.34 and 0.32 for PVDF-10wt%BN and further reduced to 0.06 and 0.28 for PVDF-10wt%BN-0.1wt%CNT at 10 N and 20 N, respectively. There was no large difference between the CoF of the pure PVDF and the PVDF-BN binary nanocomposites as 6% and 3% reduction for PVDF-10wt%BN and 83% and 15% decrease for PVDF-10wt%BN-0.1wt%CNT compared to the pure PVDF at 10 N and 20 N were obtained accordingly. The significant reduction in the CoF of the PVDF-BN-CNT ternary nanocomposites relative to their PVDF-BN binary counterparts could be credited to the high wear resistance and lubrication effect of BN [34] and the ability of the CNT to form debris by fracture, which the sliding counterface rolled over during the frictional test with reduction in the CoF [35, 36]. This has a way of preventing direct contact of the sliding counterface with the material under friction, which promotes wear resistance of such material. In addition, this also confirmed the synergetic effect of the ceramic and carbon-based nanoparticles on the enhancement of the wear resistance of polymeric materials [33]. The uniform morphology of the PVDF-BN-CNT ternary nanocomposites which was achieved by the CNT minimizing the layers-to-layers interactions of BN and the BN minimizing the walls-to-walls interactions of CNT contributed to the observed reduction in CoF. This is essential for the nanocomposites to have even distribution of frictional force to all parts of the nanocomposite system.

The wear rate of the fabricated nanocomposites for 10 N and 20 N applied loads is shown in Fig. 6. The wear rate of the nanocomposites revealed significant reduction when compared with the pure PVDF but was more pronounced for the PVDF-BN-CNT ternary nanocomposites relative to their PVDF-BN binary counterparts. For instance, the wear rate was reduced from  $5.68 \times 10^{-4}$  and  $5 \times 10^{-3}$  mm<sup>3</sup>/Nm for the pure PVDF to  $1.6 \times 10^{-6}$  and  $8 \times 10^{-6}$  mm<sup>3</sup>/Nm for PVDF-10wt%BN-0.1wt%CNT at 10 N and 20 N applied loads, respectively, which amounted to about 99.7% and 99.84% reduction, respectively. While for PVDF-10wt%BN, the wear rate was measured as  $2.15 \times 10^{-5}$  and  $4.18 \times 10^{-4}$  mm<sup>3</sup>/Nm at 10 N and 20 N, respectively.

The measured wear rate of the nanocomposites and their associated CoF showed that the PVDF-BN-CNT-based nanocomposites have better anti-wear behavior compared to the PVDF-BN binary nanocomposites. For instance, by incorporation of the BN nanoparticles into the PVDF matrix, the wear rate was reduced in comparison with the PVDF, although there was only slight difference in the wear rate of binary



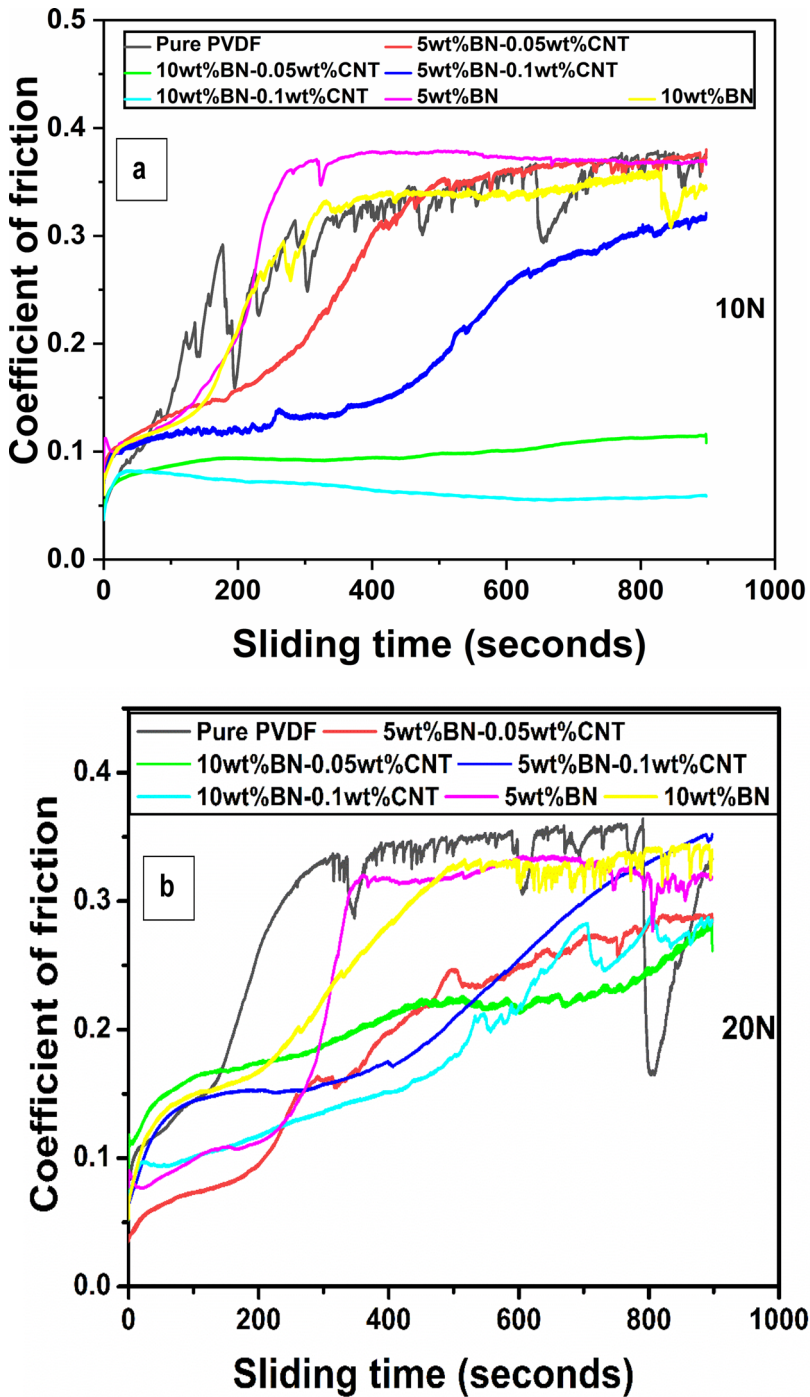


Fig. 5 Coefficient of friction of the nanocomposites at applied load of a 10 N and b 20 N

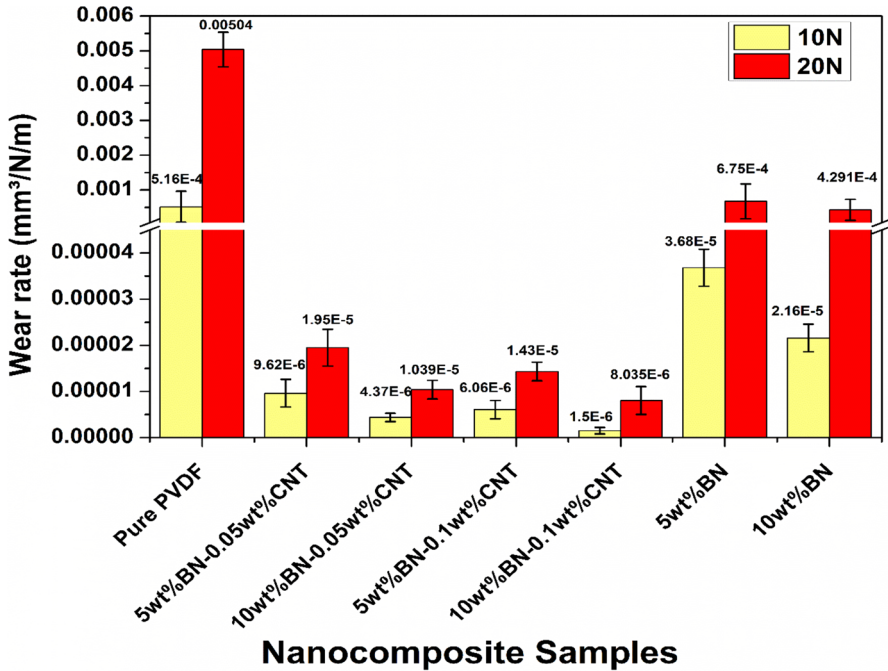
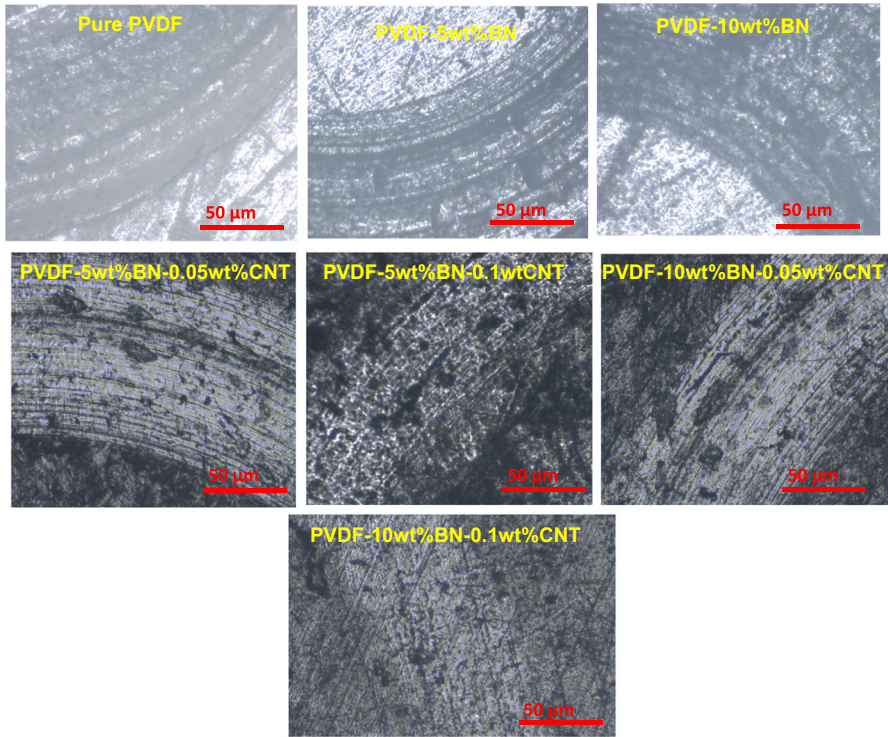


Fig. 6 Wear rate of the nanocomposites

nanocomposites containing 5 wt% and 10 wt% BN. However, on the introduction of the small content of CNT (0.05 wt% and 0.1 wt%), the wear rate significantly dropped, especially for the PVDF-10wt%BN-0.1wt%CNT nanocomposite. This is because the CNT can greatly increase the surface hardness of the nanocomposites, thereby reducing the wear rate of such nanocomposites [37]. The limited formation of agglomerated nanoparticles in the PVDF matrix due to the CNT and BN assisting each other in distribution also contributed to the enhanced wear resistance as this is essential for effective transmission of load from the matrix to the nanoparticles [38]. Absence of agglomeration of such nanoparticles in the polymer matrix could promote mechanically interlocking of the polymer matrix against slipping on the application of load, hence, resulting to improved wear resistance. The good interaction between the ceramic and carbon-based nanomaterials used in this study could also contributed to the enhanced anti-wear response of the nanocomposites [33].

Figure 7 displays the wear tracks of the nanocomposites. The pure PVDF showed a broad wear track resulting from the softness of the polymer matrix and large detachment of material during the wear test. However, the nanocomposites showed a reduction in worn scars resulting from their increase in stiffness and hardness due to the presence of the nanoparticles. Since the BN and CNT are characterized by high hardness, it was possible for the nanocomposites to have increase in hardness against removal of material during the frictional test. The nanocomposites containing the hybrid BN-CNT nanoparticles showed faint wear scars when correlate with the PVDF-BN binary nanocomposites and the pure PVDF. This indicates that the



**Fig. 7** Micrographs of the wear tracks on the nanocomposites

PVDF-BN-CNT-based nanocomposites have better resistance to wear and softening of material during the frictional test. This is expected since the CNT can form conductive network structures in the polymer matrix, which enables fast and quick conduction of frictional generated heat out the materials rather than softening of the materials [39]. Since CNT is more conductive than the BN nanoparticles, the frictional heat dissipation could have been more in PVDF-BN-CNTs based nanocomposites than the PVDF-BN-based nanocomposites, leading to the observed higher wear resistance of the PVDF-BN-CNTs group in this study. This is evidenced by the smaller debris formation and peeled materials' films from the counterface during the frictional test compared to the PVDF-BN group, which are seen as small lumps on the wear tracks of the nanocomposites.

### Nanomechanical properties

The hardness and elastic modulus of the nanocomposites were carried out using nanoindenter, and the results are presented in Fig. 8. The hardness and elastic modulus of the nanocomposites were greatly enhanced. As the concentration of BN was increase to 10 wt%, the hardness and elastic modulus also increased relative to the pure PVDF. For instance, the hardness and elastic modulus increased

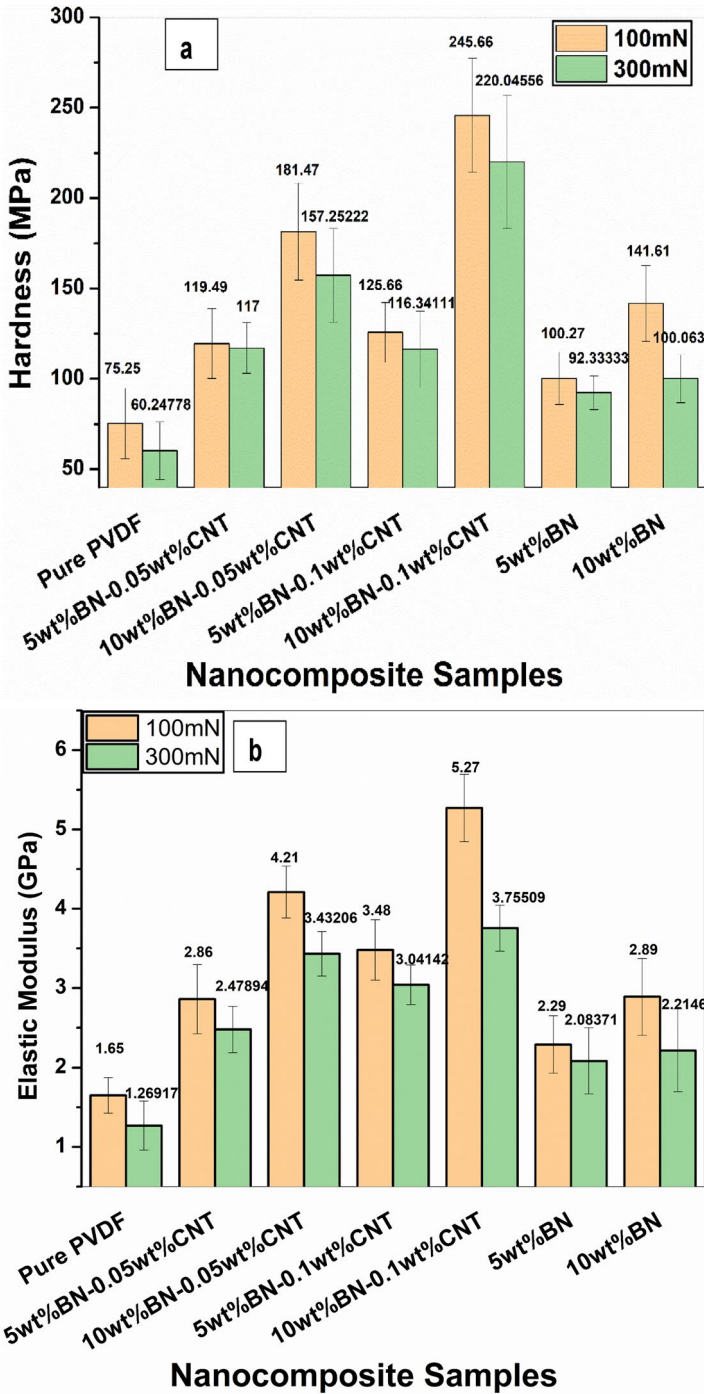


Fig. 8 a Hardness and b elastic modulus of nanocomposites

from about 100 MPa and 2.27 GPa for PVDF-5wt%BN to 141 MPa and 2.92 GPa for PVDF-10wt%BN nanocomposite, respectively, at 100-mN load. This shows that the binary nanocomposites containing 10 wt% BN increased the hardness and elastic modulus of the pure PVDF by 86% and 76%. The good mechanical properties of BN nanomaterial are responsible for the enhanced hardness and elastic modulus. However, incorporation of the CNT in the PVDF-BN binary systems further promoted the hardness and elastic modulus significantly. For instance, hardness and elastic modulus of about 246.75 MPa and 5.29 GPa were measured for the PVDF-10wt%BN-0.1wt%CNT, which amount to 225% and 219% increments at 100 mN. While the same ternary nanocomposites revealed the hardness and elastic modulus increase of about 75% and 103% compared to the PVDF-10wt%BN nanocomposite at 100-mN load. Similar results were also observed for the applied load of 300 mN as presented in Fig. 8b. This can be attributed to the high aspect ratio and large surface area of CNT, which aided in the formation of network structures in the polymer matrix with promoted hardness and elastic modulus. Hence, the significant enhanced hardness and elastic modulus of the PVDF-BN-CNT-based nanocomposites is due to network structural hardening of the polymer matrix [40]. The non-significant agglomeration of the hybrid BN-CNT nanoparticles in the PVDF matrix as revealed by the SEM micrographs in Fig. 4 also contributed to the observed nanomechanical properties. The hybrid nanoparticles having good interaction with the matrix promoted efficient transfer of stress from the matrix to the nanoparticles. Hence, the good synergy between the BN and CNT was also demonstrated through the enhanced hardness and elastic modulus of the nanocomposites. The PVDF-BN-CNT-based nanocomposites also demonstrated better interlocking of the PVDF chains, which constrained the slipping and mobility of the chains on the applications of external load with significant improvement in the mechanical properties [41].

### Displacement profile for the nanocomposites

The deformation profile of the nanocomposites at 100 mN and 300 mN is shown in Fig. 9, which presents the plot of penetration depth against penetration time. The plot shows a reduction in the penetration depth of the nanocomposites compared to the pure PVDF as the curve for the nanocomposites shifted downwards. The penetration depth showed continues increase till 20 s, it maintained 20-s holding time and retarding time of 20 s. Although the BN nanoparticles reduced the penetration depth of the PVDF-BN systems, this was more pronounced when CNT was introduced into the PVDF-BN systems. This indicates increase in stiffness and resistance to plastic deformation of the nanocomposites compared to the pure PVDF, which agrees with their high hardness and elastic modulus. The nanocomposites containing the hybrid BN-CNT nanoparticles must have experienced 3D network configurations via interpenetration of CNT and BN in the polymer matrix, which contributed to the hardening of the PVDF matrix.

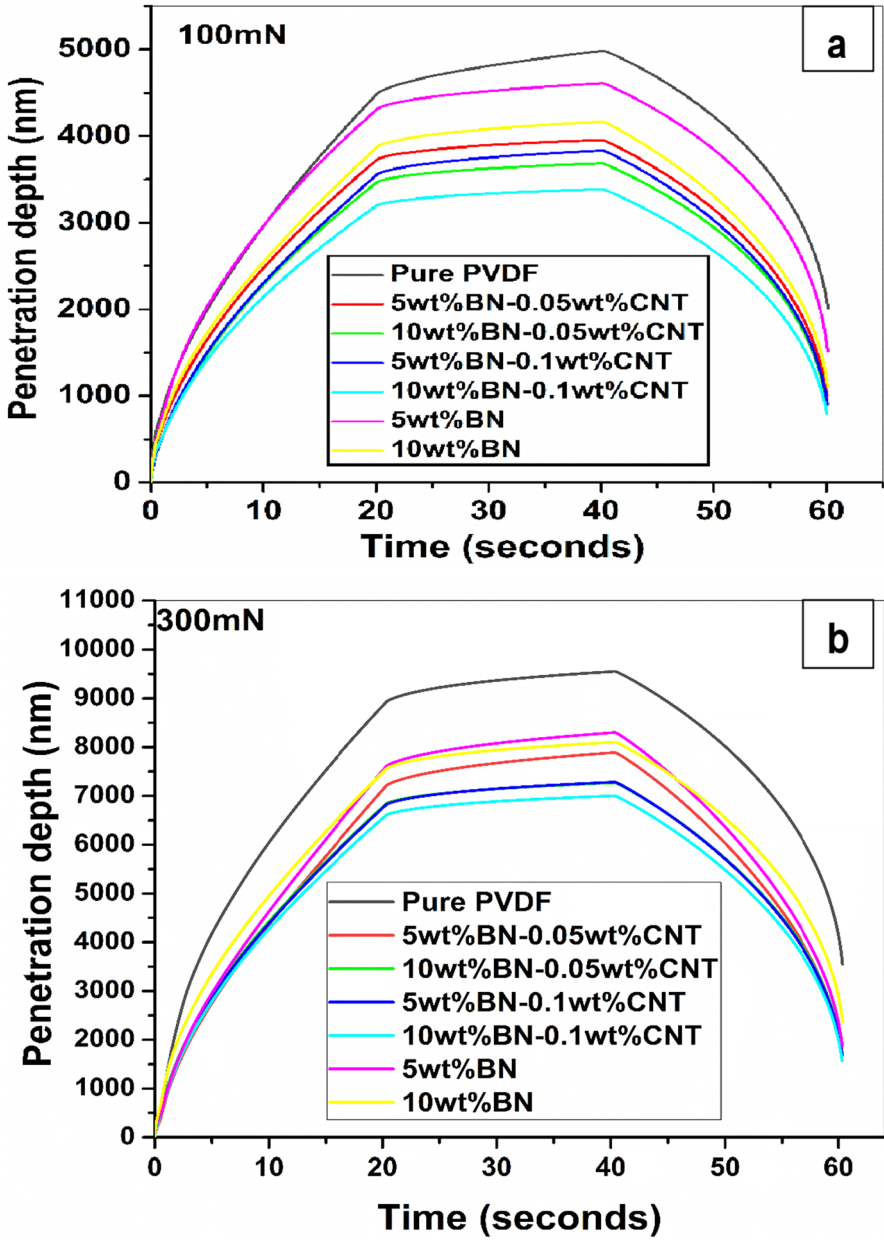


Fig. 9 Deformation profile of the nanocomposites at applied load of a 100 mN and b 300 mN

## Conclusion

In this study, CNT was used to significantly enhance the wear resistance and nanomechanical properties of PVDF-BN nanocomposites. The nanocomposites were prepared by solution mixing and hot compression processes. The SEM micrographs of the developed nanocomposites showed uniform morphology. The non-significant agglomeration of the nanoparticles was credited to CNT and BN assisting each other in the distribution in the PVDF matrix. Optimal wear rate was achieved with the PVDF-10wt%BN-0.1wt%CNT ternary nanocomposite, which showed about 99.7% and 99.84% reduction in wear rate compared to the pure PVDF at 10 N and 20 N, respectively. Also, hardness and elastic modulus of the PVDF-BN-CNT ternary nanocomposites was greatly enhanced when related to the pure PVDF and PVDF-BN binary nanocomposites. It showed an increase in hardness and elastic modulus of 225% and 219% for PVDF-10wt%BN-0.1wt%CNT compared to the pure PVDF at 100-mN applied load. In comparison with PVDF-10wt%BN nanocomposite, PVDF-10wt%BN-0.1wt%CNT showed about 75% and 103% increase. This study reveals that with only 0.05 wt% and 0.1 wt% CNTs in the PVDF-BN system, the tribological and nanomechanical properties could be further promoted. The improved properties of PVDF-BN-CNT ternary nanocomposites were as results of good synergy between CNT-BN nanoparticles, efficient transmission of stress from the polymer matrix to the hybrid nanoparticles and good mechanical interlocking of the PVDF matrix. The developed nanocomposites can find potential applications where high wear resistance and mechanical properties are required such as automobile and other mechanical components.

**Acknowledgements** We appreciate the Faculty of Engineering and the Built Environment and the Centre for Energy and Electric Power, Tshwane University of Technology, South Africa, for their supports.

**Funding** Open access funding provided by Tshwane University of Technology.

**Data availability** All data sets associated with this study are presented in this article.

## Declarations

**Conflict of interest** There is no conflict of interest to be declared in this study.

**Open Access** This article is licensed under a Creative Commons Attribution 4.0 International License, which permits use, sharing, adaptation, distribution and reproduction in any medium or format, as long as you give appropriate credit to the original author(s) and the source, provide a link to the Creative Commons licence, and indicate if changes were made. The images or other third party material in this article are included in the article's Creative Commons licence, unless indicated otherwise in a credit line to the material. If material is not included in the article's Creative Commons licence and your intended use is not permitted by statutory regulation or exceeds the permitted use, you will need to obtain permission directly from the copyright holder. To view a copy of this licence, visit <http://creativecommons.org/licenses/by/4.0/>.

## References

1. Peng H, Sun X, Weng W, Fang X (2017) 6—Energy storage devices based on polymers. *Polym Mater Energy Electron Appl*. 197–242
2. Tsonos C, Pandis C, Soin N, Sakellari D, Myrovali E, Kripotou S, Kanapitsas A, Siores E (2015) Multifunctional nanocomposites of poly (vinylidene fluoride) reinforced by carbon nanotubes and magnetite nanoparticles. *Express Polym Lett* 9(12)
3. Chan JX, Wong JF, Petrů M, Hassan A, Nirmal U, Othman N, Ilyas RA (2021) Effect of nanofillers on tribological properties of polymer nanocomposites: a review on recent development. *Polymers* 13(17):2867
4. Praveenkumara J, Madhu P, Yashas Gowda T, Sanjay M, Siengchin S (2022) A comprehensive review on the effect of synthetic filler materials on fiber-reinforced hybrid polymer composites. *J Text Instit* 113(7):1231–1239
5. Ion-Ebrasu D, Pollet BG, Caprarescu S, Chitu A, Trusca R, Niculescu V, Gabor R, Carcadea E, Varlam M, Vasile BS (2020) Graphene inclusion effect on anion-exchange membranes properties for alkaline water electrolyzers. *Int J Hydrog Energy* 45(35):17057–17066
6. Ion-Ebrașu D, Andrei RD, Enache S, Căprărescu S, Negrilă CC, Jianu C, Enache A, Boerașu I, Carcadea E, Varlam M (2021) Nitrogen functionalization of cvd grown three-dimensional graphene foam for hydrogen evolution reactions in alkaline media. *Materials* 14(17):4952
7. Kuila T, Bose S, Mishra AK, Khanra P, Kim NH, Lee JH (2012) Chemical functionalization of graphene and its applications. *Prog Mater Sci* 57(7):1061–1105. <https://doi.org/10.1016/j.pmatsci.2012.03.002>
8. Huang X, Jiang P, Tanaka T (2011) A review of dielectric polymer composites with high thermal conductivity. *IEEE Electr Insul Mag* 27(4):8–16. <https://doi.org/10.1109/mei.2011.5954064>
9. Lazau C, Nicolaescu M, Orha C, Pop A, Căprărescu S, Bandas C (2022) In situ deposition of reduced graphene oxide on Ti Foil by a facile microwave-assisted hydrothermal method. *Coatings* 12(12):1805
10. Shen X-J, Pei X-Q, Fu S-Y, Friedrich K (2013) Significantly modified tribological performance of epoxy nanocomposites at very low graphene oxide content. *Polymer* 54(3):1234–1242
11. Li C, Xiang M, Ye L (2017) Intercalation structure and highly enhancing tribological performance of monomer casting nylon-6/graphene nano-composites. *Compos A Appl Sci Manuf* 95:274–285
12. Wang J, Yi M, Shen Z, Liu L, Zhang X, Ma S (2019) Enhanced thermal and mechanical properties of poly (vinylidene fluoride) nanocomposites reinforced by liquid-exfoliated graphene. *J Macromol Sci Part A* 56(7):733–740
13. Shokrieh M, Hosseinkhani M, Naimi-Jamal M, Tourani H (2013) Nanoindentation and nanoscratch investigations on graphene-based nanocomposites. *Polym Test* 32(1):45–51
14. Onyszko M, Markowska-Szczupak A, Rakoczy R, Paszkiewicz O, Janusz J, Gorgon-Kuza A, Wenelska K, Mijowska E (2020) Few layered oxidized h-BN as nanofiller of cellulose-based paper with superior antibacterial response and enhanced mechanical/thermal performance. *Int J Mol Sci* 21(15):5396
15. Prusty K, Swain SK (2019) h-BN huddled starch reinforced polyethylhexylacrylate/polyvinyl alcohol thin films for packaging applications. *Polym Compos* 40(5):1810–1818
16. Qayyum MS, Hayat H, Matharu RK, Tabish TA, Edirisinghe M (2019) Boron nitride nanoscrolls: structure, synthesis, and applications. *Appl Phys Rev* 6(2):021310
17. Gültekin K, Uğuz G, Özel A (2021) Improvements of the structural, thermal, and mechanical properties of structural adhesive with functionalized boron nitride nanoparticles. *J Appl Polym Sci* 138(21):50491
18. Ghosh B, Xu F, Grant DM, Giangrande P, Gerada C, George MW, Hou X (2020) Highly ordered BN $\perp$ -BN $\perp$  stacking structure for improved thermally conductive polymer composites. *Adv Electron Mater* 6(11):2000627
19. Joy J, George E, Thomas S, Anas S (2020) Effect of filler loading on polymer chain confinement and thermomechanical properties of epoxy/boron nitride (h-BN) nanocomposites. *New J Chem* 44(11):4494–4503
20. Abe JO, Popoola OM, Popoola AP (2023) Assessment of nanomechanical and tribological performance of refractory nitride-reinforced titanium alloy matrix composites developed by spark plasma sintering. *JOM* 75(3):791–805



21. Norizan MN, Moklis MH, Demon SZN, Halim NA, Samsuri A, Mohamad IS, Knight VF, Abdullah N (2020) Carbon nanotubes: functionalisation and their application in chemical sensors. *RSC Adv* 10(71):43704–43732
22. Kumar A, Sharma K, Dixit AR (2021) A review on the mechanical properties of polymer composites reinforced by carbon nanotubes and graphene. *Carbon Lett* 31(2):149–165
23. Papageorgiou DG, Li Z, Liu M, Kinloch IA, Young RJ (2020) Mechanisms of mechanical reinforcement by graphene and carbon nanotubes in polymer nanocomposites. *Nanoscale* 12(4):2228–2267
24. Azimpour-Shishevan F, Akbulut H, Mohtadi-Bonab M (2020) Synergetic effects of carbon nanotube and graphene addition on thermo-mechanical properties and vibrational behavior of twill carbon fiber reinforced polymer composites. *Polym Test* 90:106745
25. Sharma S, Pathak AK, Singh VN, Teotia S, Dhakate S, Singh B (2018) Excellent mechanical properties of long multiwalled carbon nanotube bridged Kevlar fabric. *Carbon* 137:104–117
26. Ulus H, Üstün T, Eskizeybek V, Şahin ÖS, Avcı A, Ekrem M (2014) Boron nitride-MWCNT/epoxy hybrid nanocomposites: preparation and mechanical properties. *Appl Surf Sci* 318:37–42
27. Li J-S, Zhang C-R, Li B (2011) Preparation and characterization of boron nitride coatings on carbon fibers from borazine by chemical vapor deposition. *Appl Surf Sci* 257(17):7752–7757
28. Zheng M, Gu Y, Xu Z, Liu Y (2007) Synthesis and characterization of boron nitride nanoropes. *Mater Lett* 61(8–9):1943–1945
29. Li Y, Yang M, Xu B, Sun Q, Zhang W, Zhang Y, Meng F (2018) Synthesis, structure and antioxidant performance of boron nitride (hexagonal) layers coating on carbon nanotubes (multi-walled). *Appl Surf Sci* 450:284–291
30. Yu J, Jiang P, Wu C, Wang L, Wu X (2011) Graphene nanocomposites based on poly (vinylidene fluoride): structure and properties. *Polym Compos* 32(10):1483–1491
31. Meng N, Mao R, Tu W, Odolczyk K, Zhang Q, Bilotti E, Reece MJ (2017) Crystallization kinetics and enhanced dielectric properties of free standing lead-free PVDF based composite films. *Polymer* 121:88–96
32. Hu B, Guo H, Wang Q, Zhang W, Song S, Li X, Li Y, Li B (2020) Enhanced thermal conductivity by constructing 3D-networks in poly (vinylidene fluoride) composites via positively charged hexagonal boron nitride and silica coated carbon nanotubes. *Compos A Appl Sci Manuf* 137:106038
33. Chen B, Li X, Jia Y, Xu L, Liang H, Li X, Yang J, Li C, Yan F (2018) Fabrication of ternary hybrid of carbon nanotubes/graphene oxide/MoS<sub>2</sub> and its enhancement on the tribological properties of epoxy composite coatings. *Compos A Appl Sci Manuf* 115:157–165
34. Xie C, Wang K (2021) Synergistic modification of the tribological properties of polytetrafluoroethylene with polyimide and boron nitride. *Friction* 9:1474–1491
35. Min C, Liu D, Shen C, Zhang Q, Song H, Li S, Shen X, Zhu M, Zhang K (2018) Unique synergistic effects of graphene oxide and carbon nanotube hybrids on the tribological properties of polyimide nanocomposites. *Tribol Int* 117:217–224
36. Gandhi RA, Palanikumar K, Raguath B, Davim JP (2013) Role of carbon nanotubes (CNTs) in improving wear properties of polypropylene (PP) in dry sliding condition. *Mater Des* 48:52–57
37. King SG, McCafferty L, Stolojan V, Silva SRP (2015) Highly aligned arrays of super resilient carbon nanotubes by steam purification. *Carbon* 84:130–137
38. Dike AS, Mindivan F, Mindivan H (2014) Mechanical and tribological performances of polypropylene composites containing multi-walled carbon nanotubes. *Int J Surf Sci Eng* 8(4):292–301
39. Mertens AJ, Senthilvelan S (2018) Mechanical and tribological properties of carbon nanotube reinforced polypropylene composites. *J Mater Des Appl* 232(8):669–680
40. Bhattacharyya A, Chen S, Zhu M (2014) Graphene reinforced ultra high molecular weight polyethylene with improved tensile strength and creep resistance properties. *Express Polym Lett* 8(2):74–84
41. Karsli NG, Aytac A (2013) Tensile and thermomechanical properties of short carbon fiber reinforced polyamide 6 composites. *Compos B Eng* 51:270–275